Published in final edited form as:
Free Radic Biol Med. 2010 October 15; 49(7): 1238–1253. doi:10.1016/j.freeradbiomed.2010.07.020.

Cardiac Overexpression of Insulin-Like Growth Factor I (IGF-1) Attenuates Chronic Alcohol Intake-Induced Myocardial Contractile Dysfunction But Not Hypertrophy: Role of Akt, mTOR, GSK3β and PTEN

Bingfang Zhang[1,2,*], **Subat Turdi**[2,*], **Quan Li**[3,*], **Faye L. Lopez**[4], **Anna R. Eason**[2], **Piero Anversa**[5], and **Jun Ren**[2,4]

[1] Department of Geriatrics, Xijing Hospital, Fourth Military Medical University, Xi'an, China 710032

[2] Center for Cardiovascular Research and Alternative Medicine, University of Wyoming College of Health Sciences, Laramie, WY 82071

[3] Department of Anesthesiology, Shanghai Tenth People's Hospital, Tongji University School of Medicine, Shanghai, China 200072

[4] University of North Dakota School of Medicine and Health Sciences, Grand Forks, ND 58201

[5] Departments of Anesthesia and Medicine and Cardiovascular Division, Brigham and Women's Hospital, Harvard Medical School, Boston, MA 02115

Abstract

Chronic alcohol intake leads to the development of alcoholic cardiomyopathy manifested by cardiac hypertrophy and contractile dysfunction. This study was designed to examine the effect of transgenic overexpression of insulin-like growth factor I (IGF-1) on alcohol-induced cardiac contractile dysfunction. Wild-type FVB and cardiac-specific IGF-1 mice were placed on a 4% alcohol or control diet for 16 weeks. Cardiac geometry and mechanical function were evaluated by echocardiography, cardiomyocyte and intracellular Ca^{2+} properties. Histological analyses for cardiac fibrosis and apoptosis were evaluated by Masson trichrome staining and TUNEL assay, respectively. Expression and/or phosphorylation of Cu/Zn superoxide dismutase (SOD1), Ca^{2+} handling proteins, key signaling molecules for survival including Akt, mTOR, GSK3β, Foxo3a and the negative regulator of Akt phosphatase and tensin homolog on chromosome ten (PTEN) as well as mitochondrial proteins UCP-2 and PGC1α were evaluated by western blot analysis. Chronic alcohol intake led to cardiac hypertrophy, interstitial fibrosis, reduced mitochondrial number, compromised cardiac contractile function and intracellular Ca^{2+} handling, decreased SOD1 expression, elevated superoxide production and overt apoptosis, all of which with the exception of cardiac hypertrophy were abrogated by the IGF-1 transgene. Immunoblotting data showed reduced phosphorylation of Akt, mTOR, GSK3β and Foxo3a, upregulated Foxo3a and PTEN, as well as dampened SERCA2a, PGC1α and UCP-2 following alcohol intake. All these

Corresponding Author: Dr. Jun Ren, Professor Center for Cardiovascular Research and Alternative Medicine & Division of Pharmaceutical Sciences, University of Wyoming, Laramie, WY 82071 Tel: (307)-766-6131; Fax: (307)-766-2953; jren@uwyo.edu.
*Equal contribution

alcohol-induced changes in survival and mitochondrial proteins were alleviated by IGF-1. Taken together, these data favor a beneficial role of IGF-1 in alcohol-induced myocardial contractile dysfunction independent of cardiac hypertrophy.

Keywords

alcohol; cardiac hypertrophy; contractile function; intracellular Ca^{2+}; Akt; mTOR; GSK3β; Foxo3a

INTRODUCTION

Although light to moderate alcohol intake is beneficial to cardiovascular health, chronic alcohol use often result in cardiac dysfunction and arrhythmias . Almost one out of every three alcoholics display some degree of heart problems manifested as alcoholic cardiomyopathy, a dilated heart muscle disease discernable by cardiac hypertrophy, myofibrillary disruption, reduced contractility, prolonged relaxation, decreased ejection fraction and stroke volume . Up-to-date, several hypotheses have been postulated for the pathogenesis of alcoholic heart injury including direct ethanol toxicity, impaired intracellular Ca^{2+} homeostasis, buildup of fatty acid ethyl esters and free radicals . Among such, chronic alcohol intake-triggered oxidative stress, compromised antioxidant defense capacity and subsequently interrupted cardiac protein synthesis, cardiac geometry and myocardial contractile function have drawn the most attention in the pathogenesis of alcoholic myopathic injury . Maintenance of oxidant balance plays a crucial role in the physiological heart performance . Compelling evidence from our laboratory and others has indicated that oxidative damage and loss of antioxidant defense following alcohol (ethanol) exposure contribute to cardiac excitation-contraction coupling defect . Recent finding from our lab further depicted a rather beneficial role of the heavy metal scavenger metallothionein against the development of alcoholic cardiomyopathy . However, limited information is available with regards to the impact of intrinsic antioxidant capacity from natural-occurring enzymes and growth factors on alcohol-induced myocardial injury. Therefore the aim of this study was to evaluate the effect of transgenic overexpression of antioxidant insulin-like growth factor I (IGF-1) on chronic alcohol intake-induced myocardial geometric and contractile alterations. Given that oxidative stress is a major risk factor for cardiac hypertrophy, fibrosis and contractile defect while the levels of intracellular reactive oxygen species (ROS) are found elevated following alcohol exposure , superoxide production, apoptosis, mitochondrial function (biogenesis and chaperon protein), cardiac histology and myocardial ultrastructure with a focus on mitochondria were evaluated in wild-type FVB and cardiac-specific overexpression of IGF-1 transgenic mice following chronic alcohol intake. In an effort to elucidate possible cellular mechanisms behind IGF-1 and/or alcohol-induced myocardial in particular diastolic function alterations, expression of key intracellular Ca^{2+} regulatory proteins including sarco(endo)plasmic reticulum Ca^{2+-}ATPase (SERCA2a), Na^{+}/Ca^{2+} exchanger and phospholamban was monitored. The IGF-1-associated post-receptor signaling molecules including Akt, mammalian target of rapamycin (mTOR), the Forkhead transcription factor Foxo3a and glycogen synthase kinase-3 β (GSK3β) , was also examined in FVB and IGF-1 myocardium following chronic alcohol exposure. Peroxisome proliferator-activated receptor γ (PPARγ) coactivator 1α (PGC1α), which stimulates mitochondrial biogenesis through induction of mitochondrial chaperon uncoupling protein 2 (UCP-2), plays an essential role in the maintenance of mitochondrial function, glucose, lipid and energy metabolism in myocardium . In addition, Akt signaling is under the negative control of phosphatase and tensin homologue on chromosome ten (PTEN) to participate in the pathophysiology of a variety of diseases including myocardial hypertrophy, heart failure and preconditioning , expression of PGC1α, UCP-2, PTEN and

the superoxide catalytic enzyme Cu/Zn-superoxide dismutase (SOD1) was scrutinized in FVB and IGF-1 mice following chronic alcohol administration.

MATERIALS AND METHODS

Experimental animals and chronic alcohol intake

The experimental protocol described in this study was approved by the Animal Use and Care Committees at the University of North Dakota (Grand Forks, ND, USA) and the University of Wyoming (Laramie, WY, USA). Male mice with cardiac-specific overexpression of IGF-1 were used as described earlier . FVB littermates were used as wild-type. The pigmentation of fur color was used as a marker for transgenic overexpression of IGF-1 (light brown) or FVB (white) identification. All mice were housed in a temperature-controlled room under a 12hr/12hr-light/dark and allowed access to tap water *ad libitum*. Eight month-old adult male FVB and IGF-1 mice were introduced to a nutritionally complete liquid diet (Shake & Pour Bioserv Inc., Frenchtown, NJ, USA) for a one-week acclimation period. The use of a liquid diet is based on the scenario that ethanol self-administration results in less nutritional deficiencies and less stress to the animals in comparison to forced-feeding regimens, intravenous administration or aerosolized inhalation . Upon completion of the acclimation period, half of the FVB and IGF-1 mice were maintained on the regular liquid diet (without ethanol), and the remaining half began a 16-week period of isocaloric 4% (vol/vol) ethanol diet feeding. An isocaloric pair-feeding regimen was employed to eliminate the possibility of nutritional deficits. FVB or IGF-1 mice were “paired” to receive either ethanol or control liquid diet. Control mice were offered the same quantity of diet ethanol-consuming mice drank the previous day .

Measurement of blood alcohol level

On the last day of diet feeding, mice were sacrificed under anesthesia (ketamine/xylazine: 3:1, 1.32 mg/kg, i.p.). Blood was collected and stored in sealed vials. A volume of 100 μl plasma from each sample was put into an autosampler vial. Six microliter of n-propanol and 194 μl H_2O were then added to the vial. Following a 20-min incubation at 50°C, 50 μl aliquot of headspace gas was removed and transferred to an Agilent 6890 Gas Chromatograph (Agilent Technologies, Inc, Wilmington, DE, USA) equipped with a flame ionization detector. Ethanol, n-propanol and other components such as acetaldehyde were separated on a 60 m VOCOL capillary column (Supelco Inc., Bellefonte, PA, USA) with film of 1.8 μm in thickness and an inner diameter of 320 μm. The carrier gas was helium at a flow rate of 18.0 ml/min. Quantitation was achieved by calibrating peak areas against those from headspace samples of known ethanol standards .

Echocardiographic assessment

Cardiac geometry and function were evaluated in anesthetized (Avertin 2.5%, 10 μl/g body weight, i.p.) mice using 2-D guided M-mode echocardiography (Sonos 5500) equipped with a 15-6 MHz linear transducer. Left ventricular (LV) anterior and posterior wall dimensions during diastole and systole were recorded from three consecutive cycles in M-mode using methods adopted by the American Society of Echocardiography. Fractional shortening was calculated from LV end-diastolic (EDD) and end-systolic (ESD) diameters using the equation (EDD-ESD)/EDD. Echocardiographic LV mass was calculated as (LVEDD + septal wall thickness + posterior wall thickness)^3 - LVEDD^3) × 1.055, where 1.055 (mg/mm^3) is the density of myocardium. Heart rate was averaged over 10 cardiac cycles .

Cell isolation

After ketamine/xylazine sedation, hearts were rapidly removed from anesthetized mice and mounted onto a temperature-controlled (37°C) Langendorff system. After perfusing with a modified Tyrode solution (Ca^{2+} free) for 2 min, the heart was digested for 16 min with 0.9 mg/ml Liberase Blendzyme 4 (Hoffmann-La Roche Inc., Indianapolis, IN, USA). The digested heart was removed from the cannula, cut into small pieces and agitated to release cells. Extracellular Ca^{2+} was added incrementally back to 1.20 mM over a period of 30 min. Isolated cardiomyocytes were used for study within 8 hrs of isolation. Only rod-shaped cardiomyocytes with clear edges were selected for mechanical and intracellular Ca^{2+} studies .

Cell mechanics

Mechanical properties of myocytes were assessed using an IonOptix™ soft-edge system (IonOptix, Milton, MA, USA) . Myocytes were placed in a chamber mounted on the stage of an Olympus IX-70 microscope and superfused (~2 ml/min at 25°C) with a buffer containing (in mM): 131 NaCl, 4 KCl, 1 $CaCl_2$, 1 $MgCl_2$, 10 glucose and 10 HEPES. Myocytes were field stimulated at 0.5 Hz unless otherwise stated. Cell shortening and relengthening were assessed using the following indices: peak shortening (PS), time-to-PS (TPS), time-to-90% relengthening (TR_{90}) and maximal velocities of shortening/relengthening (± dL/dt). In the case of altering stimulus frequency from 0.1 Hz to 5.0 Hz, the steady state contraction of myocyte was achieved (usually after the first 5-6 beats) before PS was recorded.

Intracellular Ca^{2+} transients

Myocytes were loaded with fura-2/AM (0.5 μM) for 15 min, and fluorescence measurements were recorded with a dual-excitation fluorescence photomultiplier system (IonOptix) . Myocytes were placed in a chamber on an Olympus IX-70 inverted microscope (25°C) and imaged through a Fluor 40x oil objective. Cells were exposed to light emitted by a 75W lamp and passed through either a 360 or a 380 nm filter. Fluorescence emissions were detected between 480-520 nm by a photomultiplier tube after first illuminating cells at 360 nm for 0.5 sec then at 380 nm for the duration of the recording protocol (333 Hz sampling rate). Qualitative changes in intracellular Ca^{2+} levels were inferred from the ratio of fura-2-fluorescence intensity (FFI) at both wavelengths (360/380). Fluorescence decay time was fitted into either single or bi-exponential equation as an indicator for intracellular Ca^{2+} clearing.

Masson trichrome staining

Mice were euthanized and hearts were harvested and sliced at the mid-ventricular level followed by fixation with normal buffered formalin. Paraffin-embedded tranverse sections were cut in 5-μm in thickness and stained with Masson trichrome. The sections were photographed with a 40× objective of an Olympus BX-51 microscope equipped with an Olympus MaguaFire SP digital camera. Five random fields from each section (3 sections per mouse) were assessed for fibrosis. To determine fibrotic area, pixel counts of blue stained fibers were quantified using Color range and Histogram commands in Photoshop. Fibrotic area was calculated by dividing the pixels of blue stained area to total pixels of non-white area .

Transmission electron microscopy

Left ventricle was fixed with 2.5% glutaraldehyde/1.2% acrolein in fixative buffer (0.1 M cacodylate, 0.1 M sucrose, pH 7.4) and 1% osmium tetroxide, followed by 1% uranyl acetate, dehydrated through a graded series of ethanol concentrations before being embedded in LX112 resin (LADD Research Industries, Burlington VT, USA). Ultra thin

sections (~50 nm) were cut on the ultramicrotome, stained with uranyl acetate, followed by lead citrate, and viewed on a Hitachi H-7000 Transmission Electron Microscope equipped with a 4K × 4K cooled CCO digital camera. Quantitative analyses of mitochondrial size and mitochondrial density were carried out at a magnification of 10,000 ×. An average of 6-7 visual fields was evaluated for each mouse heart. A total of 3 mice was used per group .

Intracellular fluorescence measurement of superoxide (O_2^-)

Intracellular O_2^- was monitored by changes in fluorescence intensity resulting from intracellular probe oxidation . In brief, cardiomyocytes were loaded with 5 μM dihydroethidium (DHE) (Molecular Probes, Eugene, OR, USA) for 30 min at 37°C and washed with PBS buffer. Cells were sampled randomly using an Olympus BX-51 microscope equipped with Olympus MagnaFire™ SP digital camera and ImagePro image analysis software (Media Cybernetics, Silver Spring, MD, USA). Fluorescence was calibrated with InSpeck microspheres (Molecular Probes). An average of 100 cells was evaluated using the grid crossing method in 15 visual fields per isolation.

Caspase-3 assay

Tissue homogenates were centrifuged (10,000 *g* at 4°C, 10 min) and pellets were lysed in 100 μl of ice-cold cell lysis buffer [50 mM HEPES, pH 7.4, 0.1% CHAPS, 1 mM dithiothreitol (DTT), 0.1 mM EDTA, 0.1% NP40]. The assay was carried out in a 96-well plate with each well containing 30 μl cell lysate, 70 μl of assay buffer (50 mM HEPES, 0.1% CHAPS, 100 mM NaCl, 10 mM DTT and 1 mM EDTA) and 20 μl of caspase-3 colorimetric substrate Ac-DEVD-pNA (Sigma). The 96-well plate was incubated at 37°C for 1 hr, during which time the caspase in the sample was allowed to cleave the chromophore p-NA from the substrate molecule. Absorbency was detected at 405 nm with caspase-3 activity being proportional to color reaction. Protein content was determined using the Bradford method. The caspase-3 activity was expressed as picomoles of pNA released per μg of protein per minute .

TUNEL assay

TUNEL staining of myonuclei positive for DNA strand breaks were determined using a fluorescence detection kit (Roche, Indianapolis, IN, USA) and fluorescence microscopy. Briefly, paraffin-embedded sections (5 μm) were deparaffinized and rehydrated. The sections were then incubated with Proteinase K solution at room temperature for 30 min. TUNEL reaction mixture containing terminal deoxynucleotidyl transferase (TdT), fluorescein-dUTP was added to the sections in 50-μl drops and incubated for 60 min at 37°C in a humidified chamber in the dark. The sections were rinsed three times in PBS for 5 min each. Following embedding, sections were visualized with an Olympus BX-51 microscope equipped with an Olympus MaguaFire SP digital camera. DNase I and label solution were used as positive and negative controls. To determine the percentage of apoptotic cells, micrographs of TUNEL-positive and DAPI-stained nuclei were captured using an Olympus fluorescence microscope and counted using the ImageJ software (ImageJ version 1.43r; NIH) from 15 random fields at 400× magnification At least three hundred cells were counted in each field .

Western blot analysis

Myocardial protein was prepared as described . Samples containing equal amount of proteins were separated on 10% SDS-polyacrylamide gels in a minigel apparatus (Mini-PROTEAN II, Bio-Rad Laboratories, Inc, Hercules, CA, USA) and transferred to nitrocellulose membranes. The membranes were blocked with 5% milk in TBS-T, and were incubated overnight at 4°C with anti-Akt, anti-phosphorylated Akt (pAkt, Thr308), anti-

mTOR, anti-phosphorylated mTOR (pmTOR, Ser2448), anti-Foxo3a, anti-phosphorylated Foxo3a (pFoxo3a, Thr32), anti-GSK-3β, anti-pGSK-3β (Ser9), anti-PTEN, anti-UCP-2, anti-PGC1α, anti-SOD1, anti-SERCA2a, anti-Na^+/Ca^{2+} exchanger and anti-phospholamban antibodies. After immunoblotting, the film was scanned and the intensity of immunoblot bands was detected with a Bio-Rad Calibrated Densitometer. GAPDH was used as the loading control.

Data analysis

Data were Mean ± SEM. Statistical significance ($p < 0.05$) for each variable was estimated by a one-way analysis of variance (ANOVA) followed by a Tukey's *post hoc* analysis.

RESULTS

General features and echocardiographic properties of FVB and IGF-1 mice fed with alcohol

Chronic alcohol intake did not affect body, liver and kidney weights although the heart was significantly enlarged in comparison with the control group. IGF-1 did not affect body or organ weights in the presence or absence of chronic alcohol intake. Blood alcohol levels were significantly elevated in a similar manner in alcohol consuming FVB and IGF-1 mice compared with the non-alcohol consuming mice (undetectable levels). Heart rate was comparable among all groups (Table 1). Echocardiographic test revealed comparable left ventricular (LV) wall thickness among all groups. Chronic alcohol intake significantly increased ESD, EDD and LV mass (absolute or normalized value) while decreasing fractional shortening in FVB mice. IGF-1 overexpression itself failed to affect ESD and fractional shortening although it overtly increased EDD and LV mass (absolute or normalized value). Interestingly, the IGF-1 transgene reconciled chronic alcohol intake-induced decrease in fractional shortening without affecting alcohol-induced cardiac geometric effect especially cardiac hypertrophy (Fig. 1).

Effect of alcohol intake on mechanical and intracellular Ca^{2+} properties in cardiomyocytes

Chronic alcohol intake had no significant effect on cell phenotype (data now shown). The resting cell length was comparable between FVB and IGF-1 groups regardless of alcohol intake. Cardiomyocytes from the alcohol consuming FVB mice displayed significantly depressed PS, reduced ± dL/dt and prolonged TR_{90} associated with normal TPS. Interestingly, cardiac-specific overexpression of IGF-1 abrogated alcohol-induced mechanical alterations without eliciting any effect by itself (Fig. 2). Fig. 3A-D shows that alcohol intake significantly depressed electrically-stimulated increased in fura-2 fluorescence intensity (ΔFFI) and prolonged intracellular Ca^{2+} decay (either single or bi-exponential decay) without affecting baseline FFI. Although IGF-1 transgene itself did not affect these intracellular Ca^{2+} parameters, it abolished alcohol-induced decrease in ΔFFI and prolongation in intracellular Ca^{2+} decay without affecting baseline intracellular Ca^{2+} levels.

Effect of alcohol ingestion and IGF-1 on peak shortening-stimulus frequency relationship

Mouse hearts beat at high frequencies (> 400/min at 37°C), whereas our baseline stimulus was 0.5 Hz (30 beats/min). To investigate possible derangement of cardiac excitation-contraction coupling at higher frequencies, stimulating frequency was increased stepwise from 0.1 Hz to 5.0 Hz (300 beat/min) and PS was recorded after cardiomyocyte shortening had reached a steady-state. Cells were initially stimulated to contract at 0.5 Hz for 5 min to ensure steady-state before commencing the frequency response protocol. The PS value was normalized to that obtained at 0.1 Hz of the same cell. Myocytes from the alcohol consuming FVB mice exhibited significantly steeper negative staircase in PS with increasing stimulus frequencies (0.5 to 5.0 Hz), indicating decreased stress tolerance. While IGF-1

transgene failed to affect the peak shortening amplitude-stimulus frequency relationship in the absence of alcohol, it significantly alleviated alcohol-induced decline in peak shortening in response to increased stimulus frequencies (Fig. 3E).

Effect of chronic alcohol intake and IGF-1 on myocardial histology

To examine the effect of IGF-1 overexpression on alcohol-induced cardiac fibrosis, if any, Masson trichrome staining was performed in FVB and IGF-1 mice with or without chronic alcohol intake. Our results shown in Fig. 4 reveal that chronic alcohol intake elicits interstitial fibrosis in subepicardial regions of myocardium from FVB mice compared to those from the control hearts. Consistent with its effect on myocardial contraction following chronic alcohol intake, IGF-1 overexpression abrogated chronic alcohol intake-induced interstitial fibrosis.

Effect of chronic alcohol intake and IGF-1 on electron microscopic characteristics of hearts

In the absence of alcohol exposure, no obvious ultrastructural difference was discernable in cardiac samples between FVB and IGF-1 groups (Fig. 5A&B). Chronic alcohol exposure triggered focal damage in FVB hearts characterized by loss of mitochondrial density (Fig. 5C). Consistent with the mechanical observations, IGF-1 transgene negated chronic alcohol intake-induced cardiac ultrastructural change (Fig. 5D). Myocardial tissues from IGF-1 mice consuming alcohol chronically were ultrastructurally indistinguishable from non-alcohol consuming mice. Quantitative analysis revealed that chronic alcohol intake significantly reduced the density but not size of mitochondria in FVB hearts, the effect of which was nullified by IGF-1 (Fig. 5E&F).

Effects of IGF-1 on alcohol-induced superoxide production, SOD1 expression and apoptosis

To examine the potential mechanism of action(s) behind IGF-1-elicited protection against alcoholic cardiomyopathy, superoxide levels and apoptosis were examined in cardiomyocytes from FVB and IGF-1 mice consuming control or alcohol diets. Given the crucial role of Cu/Zn superoxide dismutase (SOD-1) in catalysis of superoxide radicals and cytoprotection against oxidative stress , SOD1 expression was assessed by western blot. Results shown in Fig. 6 indicate that superoxide production and caspase-3 activity were both significantly elevated in the alcohol-fed FVB mice. Coinciding with the alcohol intake/IGF-1-induced changes in superoxide production, chronic alcohol intake significantly downregulated the expression of SOD1 in the hearts. Although IGF-1 itself did not affect superoxide production, SOD1 expression and caspase activity, it ablated chronic alcohol intake-induced changes in superoxide production, SOD1 expression and apoptosis. In line with the caspase-3 data, TUNEL assay also revealed that IGF-1 significantly attenuated chronic alcohol intake-induced myocardial apoptosis without eliciting any effect by itself (Fig. 7).

Western blot analysis for SERCA2a, Na^+/Ca^{2+} exchanger and phospholamban

To explore the possible mechanism behind IGF-1 and/or alcohol-induced responses on diastolic function in particular intracellular Ca^{2+} homeostasis, western blot was performed to assess the levels of the essential intracellular Ca^{2+} regulatory proteins SERCA2a, Na^+/Ca^{2+} exchanger and phospholamban . Our data shown in Fig. 8 demonstrated that chronic alcohol intake significantly downregulated the expression of SERCA2a without affecting the levels of Na^+/Ca^{2+} exchanger and phospholamban in FVB mice. Although IGF-1 transgene itself did not alter the expression of SERCA2a, Na^+-Ca^{2+} exchanger and phospholamban, it

obliterated alcohol-induced change in SERCA2a without affecting Na^+/Ca^{2+} exchanger and phospholamban.

Western blot analysis for Akt, mTOR, Foxo3a and GSK3β

Western blot analysis showed that chronic alcohol administration significantly reduced phosphorylation of Akt and mTOR (either absolute value or normalized to pan protein) without affecting the expression of Akt and mTOR. IGF-1 itself enhanced Akt phosphorylation (absolute or normalized to pan Akt) without affecting total Akt, total and phosphorylated mTOR. Similar to its action on myocardial contractile function, IGF-1 reconciled chronic alcohol intake-induced loss of phosphorylation in Akt and mTOR (Fig. 9). We further examined the Akt downstream signaling Fox3a and GSK3β in FVB and IGF-1 murine hearts following chronic alcohol exposure. Our immunoblotting data revealed that chronic alcohol intake significantly enhanced expression of Foxo3a but not GSK3β and reduced phosphorylation of Foxo3a and GSK3β (either absolute or normalized value). Although IGF-1 itself failed to affect the expression of pan or phosphorylated Foxo3a and GSK3β, it ablated chronic alcohol-induced upregulation of pan Foxo3a and decrease in the phosphorylation in Foxo3a and GSK3β (Fig. 10).

Western Blot for PTEN, UCP-2 and PGC1α

Our Western blot analysis further revealed that chronic alcohol administration overtly upregulated the negative regulator of Akt - PTEN and downregulated the mitochondrial chaperon UCP-2 and the mitochondrial biogenesis cofactor PGC1α, the effect of which was abolished by transgenic overexpression of IGF-1. IGF-1 itself failed to affect the expression of PTEN, UCP-2 and PGC1α by itself (Fig. 11).

DISCUSSION

Data from the current study revealed that the antioxidant IGF-1 abrogated chronic alcohol intake-induced myocardial contractile dysfunction, intracellular Ca^{2+} derangement, dampened myocyte shortening-frequency response, interstitial fibrosis, superoxide production and apoptosis without affecting chronic alcohol intake-induced cardiac hypertrophy and geometric alteration. Moreover, IGF-1 rescued chronic alcohol intake-induced loss in the phosphorylation of essential cardiac survival proteins including Akt, mTOR, Foxo3a and GSK3β. Our data further revealed overtly upregulated expression of the tumor suppressor PTEN, decreased mitochondrial number, downregulated expression of the mitochondrial chaperon UCP-2 and the mitochondrial biogenesis cofactor PGC1α following chronic alcohol intake, the effect of which was reconciled by IGF-1. Collectively, these findings have demonstrated the beneficial role of IGF-1 in chronic alcoholism-induced myocardial contractile and intracellular Ca^{2+} dysfunction independent of cardiac hypertrophy and geometric changes. Our results favor a beneficial role of IGF-1 and possibly other antioxidants in cardiac contractile and intracellular Ca^{2+} dysregulation, cardiac fibrosis, superoxide accumulation and apoptosis associated with chronic alcohol administration.

The hallmarks of alcoholic cardiomyopathy are characterized by cardiac hypertrophy and compromised myocardial contractility . This is supported by our current observation of enlarged ventricular size (EDD and ESD although not wall thickness), ventricular mass (absolute and normalized), decreased fractional shortening and compromised cardiomyocyte shortening capacity (decreased PS/± dL/dt and prolonged TR_{90}) in FVB mice consuming alcohol. Our findings of increased left ventricular mass and heart weight associated with the unchanged wall thickness following chronic alcohol intake favor the notion of hypertrophic geometry through dilation of ventricular chamber walls. This is in accordance with the

commonly accepted concept that alcoholic cardiomyopathy belongs to a form of dilated cardiomyopathy . Conflicting data on alcohol-induced changes in cardiac geometry have been reported with unchanged , decreased and increased ventricular wall thickness associated increased LV mass. Possible reasons for these discrepancies may include differences in the severity and duration of alcoholism, existence of other cardiac commodities, age and species of experimental subjects. Our data suggested alcohol intake-induced intracellular Ca^{2+} anomalies (decreased ΔFFI and delayed intracellular Ca^{2+} decay) may underscore cardiac contractile dysfunction following chronic alcohol ingestion, consistent with the notion of an essential role for impaired intracellular Ca^{2+} homeostasis in alcoholic cardiomyopathy . Interestingly, our data indicated exaggerated cardiac depression with increased stimulus frequency (steeper staircase) following chronic alcohol ingestion, consistent with our earlier report . Our findings of prolonged relaxation duration (TR_{90}) and intracellular Ca^{2+} decay time indicate a poor intracellular Ca^{2+} re-sequestration or Ca^{2+} cycling ability, hallmarks of diastolic dysfunction , following chronic alcohol intake. Impaired relaxation and diastolic dysfunction have been considered an early sign of alcoholic cardiomyopathy . Our results of downregulated SERCA2a expression and interstitial fibrosis in alcoholic myocardium favor a role of compromised intracellular Ca^{2+} extrusion and ventricular compliance in the development of diastolic dysfunction in alcoholism. Chronic alcohol intake is known to impair intracellular Ca^{2+} transport back into sarcoplasmic reticulum, leading to a delayed inactivation of actomyosin interaction and prolonged myocardial relaxation . Our data, however, do not favor a major role of Na^{+}-Ca^{2+} exchanger and phospholamban in impaired intracellular Ca^{2+} handling under alcoholism. In our hand, we failed to observe an alcoholism-associated liver enlargement. Hepatomegaly is one of the consequences of chronic alcohol intake although this increase in liver weight may be different depending upon species, the dose and duration of alcohol intake. Negligible increase in liver weight or size (normalized to body weight) has been reported in our lab as well as others . Last but not the least, we failed to note any change in heart rate following chronic alcohol intake. Heart rate is regulated by sympathetic and parasympathetic inputs, both of which are affected in a dose dependent manner by alcoholism . Although the mechanism behind the unchanged heart rate in our current experimental setting is unclear at this point, anesthesia (Avertin) may play a role in the sedated mice when heart rate was taken 8 hrs after the daily alcohol feeding. In line with our data, Lazarevic and colleagues found unaltered heart rate in human alcoholics .

Perhaps the most striking piece of data from our current study was that IGF-1 attenuated or abolished alcohol intake-induced myocardial, cardiomyocyte contractile and intracellular Ca^{2+} defects without affecting alcohol-induced cardiac hypertrophy and geometric alterations. Several scenarios may be considered for the beneficial effects of IGF-1 under alcoholism. First, IGF-1 may elicit its cardioprotective effect against alcoholism through scavenging free radicals and its anti-apoptotic property. Chronic alcoholism is known to trigger severe oxidative stress, apoptosis and ultimately protein damage , which is supported by our current observation of enhanced superoxide production, downregulated SOD1 level and apoptosis (caspase-3 activation and TUNEL assay) in alcohol consuming FVB group. In our hands, IGF-1 effectively lessened alcohol-induced superoxide accumulation, loss of the superoxide catalytic enzyme SOD1 and apoptosis. Secondly, IGF-1 may offer myocardial protection against chronic alcohol-induced cardiac mechanical defect through improved post-IGF-1 receptor signaling in Akt and its downstream effectors. This is supported by our observation that IGF-1 significantly improved the dampened phosphorylation of several essential post-IGF-1 receptor signals Akt, mTOR, Foxo3a and GSK3β following chronic alcohol administration. IGF-1, similar to insulin, is known to exert its biological actions through IGF-1 receptor and the post-receptor signaling molecules including Akt, mTOR, Foxo3a and GSK3β . These signaling molecules play an essential role in the maintenance of cardiac survival, structure and function. Akt is a key cell survival factor with reduced Akt

activation directly contributing to apoptosis and cardiac dysfunction . mTOR is a central regulator of protein synthesis and cell growth. Data from our current study revealed that chronic alcohol intake significantly dampened phosphorylation of Akt and mTOR without affecting pan Akt and mTOR levels, similar to our earlier result of reduced phosphorylation of Akt and mTOR following chronic alcohol intake . Our data revealed that IGF-1 transgene restored the dampened phosphorylation of Akt and mTOR following chronic alcoholism, suggesting a likely role of these cardiac survival proteins in IGF-1-elicited cardioprotective effect. Furthermore, our data revealed that chronic alcohol intake lessened phosphorylation of the Akt downstream signaling molecules Foxo3a and GSK3β. We found that chronic alcohol intake significantly upregulated the expression of the proapoptotic transcriptional factor Foxo3a associated with reduced Foxo3a inactivation (phosphorylation), the effect of which was nullified by IGF-1. Our observation of enhanced pan Foxo3a expression and reduced Foxo3a phosphorylation appears to coincide with enhanced apoptosis (caspase-3 activity and TUNEL) in chronic alcoholism. The decrease in Foxo3a and GSK3β phosphorylation is likely resulted from the dampened phosphorylation of the upstream molecule Akt. GSK-3β, a serine/threonine kinase, is inactivated by phosphorylation of Ser9 by oxidative stress and may serve as a negative regulator of cardiac hypertrophy . Our finding of enhanced pAkt/Akt, pmTOR/mTOR, pGSK3β/GSK3β and pFoxo3a/Foxo3a ratios in the alcohol consuming IGF-1 murine hearts is consistent with the pro-hypertrophic response seen in these mice. However, the reduced phosphorylated-to-pan protein ratio of Akt, mTOR, Foxo3a and GSK3β following chronic alcohol intake, in light of the cardiac hypertrophy, suggests likelihood contribution of alternate mechanism(s) to chronic alcoholism-associated cardiac hypertrophy. For example, data from our recent study suggested a role of phosphorylation of GATA4 and cAMP-response element binding (CREB) in cardiac hypertrophy following chronic alcohol intake . Last but not the least, IGF-1 transgene reversed alcohol-induced upregulation of PTEN, a negative regulator for Akt signaling . It is plausible to speculate that IGF-1-elicited offsetting effect against the alcohol-induced upregulation in PTEN may underscore the IGF-1-induced Akt activation following alcohol intake. Ethanol has been shown to impair neuronal survival due to reduced PI-3 kinase and Akt kinase activity due to inability to suppress PTEN although no information is available with regards to cardiac PTEN function in alcoholism. Our data revealed that IGF-1 increased left ventricular EDD with no change in ESD and factional shortening in the absence of alcohol intake. This apparent mismatch between fractional shortening and ventricular diameters in IGF-1 mice is somewhat similar to the scenario of the preserved ejection fraction in patients with diastolic heart failure where increased diastolic diameter is capable of nullifying overt change in factional shortening (or ejection fraction) .

IGF-1 regulates myocardial function under both physiological and pathophysiological settings . Acute IGF-1 exposure has been shown to directly improve cardiac contractile function, intracellular Ca^{2+} handling and cell survival . In particular, acute IGF-1 treatment triggers a positive inotropic response in myocardium associated with a rise in cytosolic Ca^{2+} . In cardiomyocytes from end-stage failing hearts, acute IGF-1 administration increased intracellular Ca^{2+} through opening L-type Ca^{2+} current and the reverse-mode Na^{+}-Ca^{2+} exchange . Acute IGF-1 treatment may also promote positive inotropicity through sensitizing the myofilament to Ca^{2+} without increasing intracellular Ca^{2+} levels . Other than its myocardial contractile effect, substantial data suggest the role of IGF-1 as a potent cardiomyocyte survival factor. IGF-1 significantly attenuated both serum-free and doxorubicin-induced cardiomyocyte apoptosis via attenuation of Bax and caspase-3 activation . Interestingly, these beneficial effects of IGF-1 are less pronounced with chronic endogenous overexpression of the growth factor. Although constitutive overexpression of IGF-1 may positively influence some but not all aspects of cardiomyocyte performance such as shortening velocity and cellular compliance early on in life (2.5 months of age) , cardiac

mechanical function, intracellular Ca^{2+} handling and cell survival were found essentially similar in cardiomyocytes between adult IGF-1 transgenic mice and the wild-type littermates . These findings suggest the complexity of myocardial effect of IGF-1 which may be influenced by age, environment and existence of certain diseases. In our current study, we failed to observe any notable effect of IGF-1 overexpression on cardiac mechanical function, intracellular Ca^{2+} property and cell survival in the absence of alcohol intake. These findings (unchanged fractional shortening, cardiomyocyte contractile function and intracellular Ca^{2+} homeostasis) in conjunction with comparable superoxide production, apoptosis and apoptotic signaling (e.g., Foxo3a and GSK3β) in IGF-1 transgenic mouse hearts, is somewhat consistent with our previous reports using the same model , indicating that chronic overexpression of IGF-1 may not significantly alter cardiac function, intracellular Ca^{2+} handling and cell survival. It may be speculated that the difference between the *in vitro* and *in vivo* experimental settings as well as the difficulty of discriminating very low degree of apoptosis at basal levels may contribute to the apparent discrepancy between acute and chronic IGF-1 response in the heart.

Our ultrastructural finding revealed reduced mitochondrial number but not size following chronic alcohol intake, consistent with the immunoblot findings of downregulated PGC1α and UCP-2. Mitochondrial damage has been demonstrated to result in apoptosis through mitochondrial pathways following chronic alcohol intake . PGC1α is known to stimulate mitochondrial biogenesis and respiration in myocardium through an induction of UCP-2 and regulation of the nuclear respiratory factors . The fact that IGF-1 transgene reversed alcohol-induced superoxide production and loss of PGC1α and UCP-2 proteins has further substantiated the critical role of mitochondria in ethanol-induced myocardial damage and IGF-1-offered protection against alcoholic cardiomyopathy. Nonetheless, it is worth mentioning that our current study cannot directly address the intimate interplay between mitochondrial damage and myocardial dysfunction under chronic alcohol intake.

Experimental limitation: It should be noteworthy that resting cell length is a rather arbitrary measure that can be influenced by various experimental settings. Sarcomere length is a much better measure of cell length although we were unable to report this index due to technical limitation. In addition, given the possible influence of mouse age in IGF-1 overexpression-induced cardiac contractile response and cell survival, the age of mice used in our study may also affect the ultimate effect of IGF-1 overexpression on the experimental indices tested under both drinking and nondrinking conditions.

In our study, we demonstrated that IGF-1 significantly alleviated chronic alcohol intake-induced myocardial contractile and intracellular Ca^{2+} dysfunction, interstitial fibrosis and apoptosis without reconciling cardiac hypertrophy and geometric changes following chronic intake. This is likely due to the pleiotropic effect of IGF-1 in addition to its potent antioxidant property. Cardiac hypertrophy following chronic alcohol intake may become maladaptive and contribute to cardiac contractile dysfunction . Data from our study revealed that the beneficial effect of IGF-1 against chronic alcohol intake is independent of cardiac geometric alterations. In light of the IGF-1-elicited protection against chronic alcohol intake-induced cardiac mechanical dysfunction, intracellular Ca^{2+} dysregulation, interstitial fibrosis, apoptosis, dampened activation of essential post-IGF-1 receptor signaling molecules as well as loss of mitochondrial density, our data favor the therapeutic value of the growth factor in aberrant myocardial function following alcohol intake. It is imperative that we understand the mitochondrial function change under chronic alcoholism so that treatment strategy may be targeted at achieving sufficient induction of mitochondrial biogenesis or chaperon within a therapeutically beneficial window.

Acknowledgments

The authors would like to acknowledge Dr. Edward C. Carlson from University of North Dakota School of Medicine and Dr. Zhaojie Zhang from University of Wyoming Microscopy Facility for their guidance in microscopic study. We also wish to thank Ms. Karissa H. LaCour, Ms. Kato Kasai and Ms. Bonnie H. Zhao from University of Wyoming College of Health Sciences for their assistance in data analysis. This work was supported in part by 1R15AA13575 and 1R01 AA013412 (JR).

Reference List

[1]. Preedy VR, Adachi J, Peters TJ, Worrall S, Parkkila S, Niemela O, Asamo M, Ueno Y, Takeda K, Yamauchi M, Sakamoto K, Takagi M, Nakajima H, Toda G. Recent advances in the pathology of alcoholic myopathy. Alcohol Clin Exp. Res. 2001; 25:54S–59S. [PubMed: 11391050]

[2]. Spies CD, Sander M, Stangl K, Fernandez-Sola J, Preedy VR, Rubin E, Andreasson S, Hanna EZ, Kox WJ. Effects of alcohol on the heart. Curr. Opin. Crit Care. 2001; 7:337–343. [PubMed: 11805530]

[3]. Lazarevic AM, Nakatani S, Neskovic AN, Marinkovic J, Yasumura Y, Stojicic D, Miyatake K, Bojic M, Popovic AD. Early changes in left ventricular function in chronic asymptomatic alcoholics: relation to the duration of heavy drinking. J Am Coll Cardiol. 2000; 35:1599–1606. [PubMed: 10807466]

[4]. Ren J, Wold LE. Mechanisms of alcoholic heart disease. Ther. Adv. Cardiovasc. Dis. 2008; 2:497–506. [PubMed: 19124444]

[5]. Preedy VR, Patel VB, Why HJ, Corbett JM, Dunn MJ, Richardon PJ. Alcohol and the heart: biochemical alterations. Cardiovasc. Res. 1996; 31:139–147. [PubMed: 8849598]

[6]. Preedy VR, Patel VB, Reilly ME, Richardson PJ, Falkous G, Mantle D. Oxidants, antioxidants and alcohol: implications for skeletal and cardiac muscle. Front Biosci. 1999; 4:e58–e66. [PubMed: 10430553]

[7]. Zhang X, Li SY, Brown RA, Ren J. Ethanol and acetaldehyde in alcoholic cardiomyopathy: from bad to ugly en route to oxidative stress. Alcohol. 2004; 32:175–186. [PubMed: 15282111]

[8]. Goldhaber JI, Qayyum MS. Oxygen free radicals and excitation-contraction coupling. Antioxid. Redox. Signal. 2000; 2:55–64. [PubMed: 11232601]

[9]. Zhang X, Klein AL, Alberle NS, Norby FL, Ren BH, Duan J, Ren J. Cardiac-specific overexpression of catalase rescues ventricular myocytes from ethanol-induced cardiac contractile defect. J. Mol. Cell Cardiol. 2003; 35:645–652. [PubMed: 12788382]

[10]. Hintz KK, Relling DP, Saari JT, Borgerding AJ, Duan J, Ren BH, Kato K, Epstein PN, Ren J. Cardiac overexpression of alcohol dehydrogenase exacerbates cardiac contractile dysfunction, lipid peroxidation, and protein damage after chronic ethanol ingestion. Alcohol Clin. Exp. Res. 2003; 27:1090–1098. [PubMed: 12878915]

[11]. Li Q, Ren J. Cardiac overexpression of metallothionein attenuates chronic alcohol intake-induced cardiomyocyte contractile dysfunction. Cardiovasc. Toxicol. 2006; 6:173–182. [PubMed: 17347528]

[12]. Li Q, Ren J. Cardiac overexpression of metallothionein rescues chronic alcohol intake-induced cardiomyocyte dysfunction: role of Akt, mammalian target of rapamycin and ribosomal p70s6 kinase. Alcohol Alcohol. 2006; 41:585–592. [PubMed: 17020909]

[13]. Catalucci D, Latronico MV, Ellingsen O, Condorelli G. Physiological myocardial hypertrophy: how and why? Front Biosci. 2008; 13:312–324. [PubMed: 17981549]

[14]. Salminen A, Kaarniranta K. Insulin/IGF-1 paradox of aging: regulation via AKT/IKK/NF-kappaB signaling. Cell Signal. 2010; 22:573–577. [PubMed: 19861158]

[15]. Wu Z, Puigserver P, Andersson U, Zhang C, Adelmant G, Mootha V, Troy A, Cinti S, Lowell B, Scarpulla RC, Spiegelman BM. Mechanisms controlling mitochondrial biogenesis and respiration through the thermogenic coactivator PGC-1. Cell. 1999; 98:115–124. [PubMed: 10412986]

[16]. Oudit GY, Penninger JM. Cardiac regulation by phosphoinositide 3-kinases and PTEN. Cardiovasc. Res. 2009; 82:250–260. [PubMed: 19147653]

[17]. Ren J, Duan J, Thomas DP, Yang X, Sreejayan N, Sowers JR, Leri A, Kajstura J, Gao F, Anversa P. IGF-I alleviates diabetes-induced RhoA activation, eNOS uncoupling, and myocardial dysfunction. Am. J. Physiol Regul. Integr. Comp Physiol. 2008; 294:R793–R802. [PubMed: 18199585]

[18]. Norby FL, Aberle NS, Kajstura J, Anversa P, Ren J. Transgenic overexpression of insulin-like growth factor I prevents streptozotocin-induced cardiac contractile dysfunction and beta-adrenergic response in ventricular myocytes. J. Endocrinol. 2004; 180:175–182. [PubMed: 14709156]

[19]. Keane B, Leonard BE. Rodent models of alcoholism: a review. Alcohol Alcohol. 1989; 24:299–309. [PubMed: 2675861]

[20]. Ren J, Brown RA. Influence of chronic alcohol ingestion on acetaldehyde-induced depression of rat cardiac contractile function. Alcohol Alcohol. 2000; 35:554–560. [PubMed: 11093961]

[21]. Ren J, Babcock SA, Li Q, Huff AF, Li SY, Doser TA. Aldehyde dehydrogenase-2 transgene ameliorates chronic alcohol ingestion-induced apoptosis in cerebral cortex. Toxicol. Lett. 2009; 187:149–156. [PubMed: 19429258]

[22]. Doser TA, Turdi S, Thomas DP, Epstein PN, Li SY, Ren J. Transgenic overexpression of aldehyde dehydrogenase-2 rescues chronic alcohol intake-induced myocardial hypertrophy and contractile dysfunction. Circulation. 2009; 119:1941–1949. [PubMed: 19332462]

[23]. Dong F, Li Q, Sreejayan N, Nunn JM, Ren J. Metallothionein prevents high-fat diet induced cardiac contractile dysfunction: role of peroxisome proliferator activated receptor gamma coactivator 1alpha and mitochondrial biogenesis. Diabetes. 2007; 56:2201–2212. [PubMed: 17575086]

[24]. Dong F, Zhang X, Ren J. Leptin regulates cardiomyocyte contractile function through endothelin-1 receptor-NADPH oxidase pathway. Hypertension. 2006; 47:222–229. [PubMed: 16380530]

[25]. Fridovich I. The biology of oxygen radicals. Science. 1978; 201:875–880. [PubMed: 210504]

[26]. Wang P, Chen H, Qin H, Sankarapandi S, Becher MW, Wong PC, Zweier JL. Overexpression of human copper, zinc-superoxide dismutase (SOD1) prevents postischemic injury. Proc. Natl. Acad. Sci. U. S. A. 1998; 95:4556–4560. [PubMed: 9539776]

[27]. Kessova IG, Ho YS, Thung S, Cederbaum AI. Alcohol-induced liver injury in mice lacking Cu, Zn-superoxide dismutase. Hepatology. 2003; 38:1136–1145. [PubMed: 14578852]

[28]. Kass DA, Bronzwaer JGF, Paulus WJ. What Mechanisms Underlie Diastolic Dysfunction in Heart Failure? Circ Res. 2004; 94:1533–1542. [PubMed: 15217918]

[29]. Patel VB, Why HJ, Richardson PJ, Preedy VR. The effects of alcohol on the heart. Adverse Drug React. Toxicol. Rev. 1997; 16:15–43. [PubMed: 9192055]

[30]. Richardson PJ, Patel VB, Preedy VR. Alcohol and the myocardium. Novartis. Found. Symp. 1998; 216:35–45. [PubMed: 9949786]

[31]. Kim SD, Bieniarz T, Esser KA, Piano MR. Cardiac structure and function after short-term ethanol consumption in rats. Alcohol. 2003; 29:21–29. [PubMed: 12657373]

[32]. Li SY, Fang CX, Aberle NS, Ren BH, Ceylan-Isik AF, Ren J. Inhibition of PI-3 kinase/Akt/mTOR, but not calcineurin signaling, reverses insulin-like growth factor I-induced protection against glucose toxicity in cardiomyocyte contractile function. J. Endocrinol. 2005; 186:491–503. [PubMed: 16135669]

[33]. Piano MR, Geenen DL, Schwertz DW, Chowdhury SA, Yuzhakova M. Long-term effects of alcohol consumption in male and female rats. Cardiovasc Toxicol. 2007; 7:247–254. [PubMed: 17990129]

[34]. Askanas A, Udoshi M, Sadjadi SA. The heart in chronic alcoholism: a noninvasive study. Am. Heart J. 1980; 99:9–16. [PubMed: 6444262]

[35]. Kupari M, Koskinen P, Suokas A, Ventila M. Left ventricular filling impairment in asymptomatic chronic alcoholics. Am J Cardiol. 1990; 66:1473–1477. [PubMed: 2251994]

[36]. Silberbauer K, Juhasz M, Ohrenberger G, Hess C. Noninvasive assessment of left ventricular diastolic function by pulsed Doppler echocardiography in young alcoholics. Cardiology. 1988; 75:431–439. [PubMed: 3067838]

[37]. Israel Y, Orrego H, Colman JC, Britton RS. Alcohol-induced hepatomegaly: pathogenesis and role in the production of portal hypertension. Fed. Proc. 1982; 41:2472–2477. [PubMed: 7084488]

[38]. Ivester P, Shively CA, Register TC, Grant KA, Reboussin DM, Cunningham CC. The effects of moderate ethanol consumption on the liver of the monkey, Macaca fascicularis. Alcohol Clin Exp. Res. 2003; 27:1831–1837. [PubMed: 14634501]

[39]. Fromenty B, Vadrot N, Massart J, Turlin B, Barri-Ova N, Lettéon P, Fautrel A, Robin MA. Chronic Ethanol Consumption Lessens the Gain of Body Weight, Liver Triglycerides, and Diabetes in Obese ob/ob Mice. Journal of Pharmacology and Experimental Therapeutics. 2009; 331:23–34. [PubMed: 19587315]

[40]. Ren J, Wold LE, Natavio M, Ren BH, Hannigan JH, Brown RA. Influence of prenatal alcohol exposure on myocardial contractile function in adult rat hearts: role of intracellular calcium and apoptosis. Alcohol Alcohol. 2002; 37:30–37. [PubMed: 11825854]

[41]. Condorelli G, Drusco A, Stassi G, Bellacosa A, Roncarati R, Iaccarino G, Russo MA, Gu Y, Dalton N, Chung C, Latronico MV, Napoli C, Sadoshima J, Croce CM, Ross J Jr. Akt induces enhanced myocardial contractility and cell size in vivo in transgenic mice. Proc. Natl. Acad. Sci. U. S. A. 2002; 99:12333–12338. [PubMed: 12237475]

[42]. Xu J, Yeon JE, Chang H, Tison G, Chen GJ, Wands J, de la MS. Ethanol impairs insulin-stimulated neuronal survival in the developing brain: role of PTEN phosphatase. J. Biol. Chem. 2003; 278:26929–26937. [PubMed: 12700235]

[43]. Sanderson JE. Diastolic heart failure or heart failure with a normal ejection fraction. Minerva Cardioangiol. 2006; 54:715–724. [PubMed: 17167383]

[44]. Ren J, Samson WK, Sowers JR. Insulin-like growth factor I as a cardiac hormone: physiological and pathophysiological implications in heart disease. J Mol. Cell Cardiol. 1999; 31:2049–2061. [PubMed: 10591031]

[45]. Ren J, Walsh MF, Hamaty M, Sowers JR, Brown RA. Altered inotropic response to IGF-I in diabetic rat heart: influence of intracellular Ca2+ and NO. Am J Physiol. 1998; 275:H823–H830. [PubMed: 9724285]

[46]. Freestone NS, Ribaric S, Mason WT. The effect of insulin-like growth factor-1 on adult rat cardiac contractility. Mol. Cell Biochem. 1996; 163-164:223–229. [PubMed: 8974061]

[47]. von Lewinski D, Voss K, Hulsmann S, Kogler H, Pieske B. Insulin-Like Growth Factor-1 Exerts Ca2+-Dependent Positive Inotropic Effects in Failing Human Myocardium. Circ Res. 2003; 92:169–176. [PubMed: 12574144]

[48]. Cittadini A, Ishiguro Y, Stromer H, Spindler M, Moses AC, Clark R, Douglas PS, Ingwall JS, Morgan JP. Insulin-like growth factor-1 but not growth hormone augments mammalian myocardial contractility by sensitizing the myofilament to Ca2+ through a wortmannin-sensitive pathway: studies in rat and ferret isolated muscles. Circ Res. 1998; 83:50–59. [PubMed: 9670918]

[49]. Suleiman MS, Singh RJ, Stewart CE. Apoptosis and the cardiac action of insulin-like growth factor I. Pharmacol. Ther. 2007; 114:278–294. [PubMed: 17499363]

[50]. Redaelli G, Malhotra A, Li B, Li P, Sonnenblick EH, Hofmann PA, Anversa P. Effects of constitutive overexpression of insulin-like growth factor-1 on the mechanical characteristics and molecular properties of ventricular myocytes. Circ Res. 1998; 82:594–603. [PubMed: 9529164]

[51]. Li Q, Ren J. Influence of cardiac-specific overexpression of insulin-like growth factor 1 on lifespan and aging-associated changes in cardiac intracellular Ca2+ homeostasis, protein damage and apoptotic protein expression. Aging Cell. 2007; 6:799–806. [PubMed: 17973971]

[52]. Li Q, Wu S, Li SY, Lopez FL, Du M, Kajstura J, Anversa P, Ren J. Cardiac-specific overexpression of insulin-like growth factor 1 attenuates aging-associated cardiac diastolic contractile dysfunction and protein damage. Am. J. Physiol Heart Circ. Physiol. 2007; 292:H1398–H1403. [PubMed: 17085535]

[53]. Guo R, Ren J. Alcohol dehydrogenase accentuates ethanol-induced myocardial dysfunction and mitochondrial damage in mice: role of mitochondrial death pathway. PLoS. One. 2010; 5:e8757. [PubMed: 20090911]

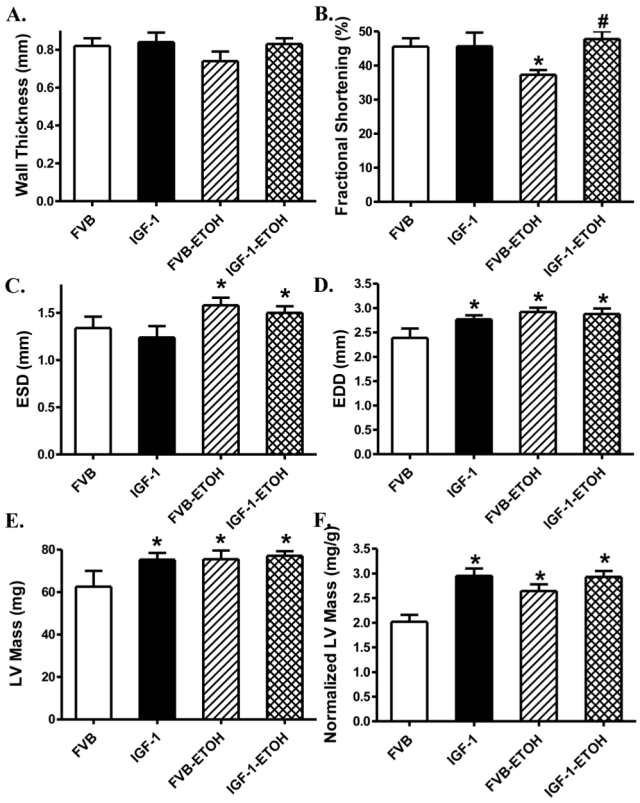

Fig. 1.

Echocardiographic properties of FVB and IGF-1 transgenic mice with or without chronic alcohol intake. (A): Left ventricular (LV) wall thickness; (B): Fractional shortening (%); (C): LV end systolic diameter (ESD); (D): LV end diastolic diameter (EDD); (E): Calculated LV mass; and (F): Normalized LV mass. Mean ± SEM, n = 8 mice per group, * $p < 0.05$ *vs.* FVB group, # $p < 0.05$ *vs.* FVB mice consuming ethanol (FVB-ETOH).

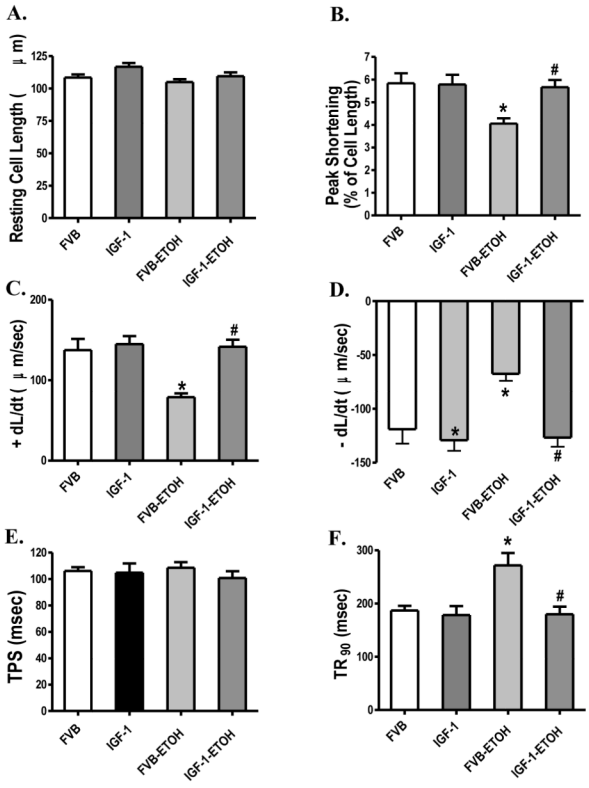

Fig. 2.

Effect of chronic alcohol intake on cell shortening/relengthening in cardiomyocytes from FVB and IGF-1 mice. (A): Resting cell length; (B). Peak shortening amplitude (% of resting cell length); (C): Maximal velocity of shortening (+ dL/dt); (D). Maximal velocity of relengthening (− dL/dt); (E). Time-to-peak shortening (TPS); and (F): Time-to-90% relengthening (TR_{90}). Mean ± SEM, n = 69 - 70 cells per group. * $p < 0.05$ *vs.* FVB group, # $p < 0.05$ *vs*. FVB mice consuming ethanol (FVB-ETOH).

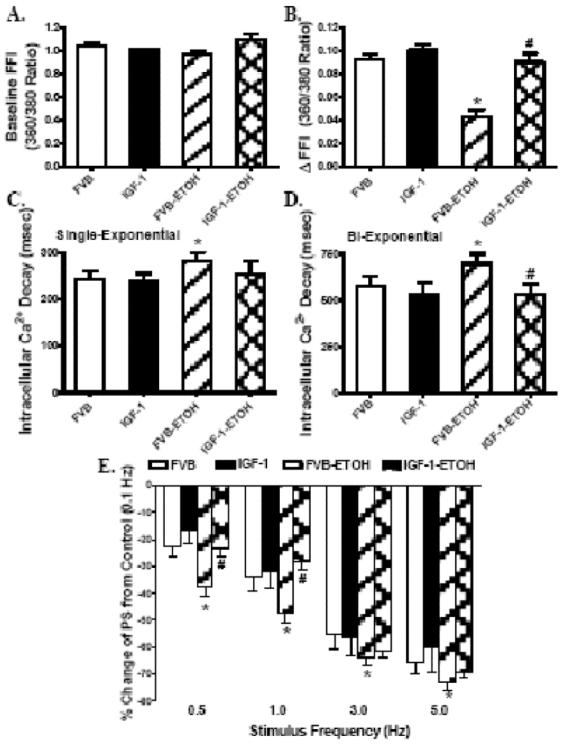

Fig. 3.

Effect of chronic alcohol intake on intracellular Ca^{2+} transients and stimulus frequency-peak shortening (PS) response in cardiomyocytes from FVB and IGF-1 mice. (A): Baseline intracellular Ca^{2+} fura-2 fluorescent intensity (FFI); (B) Change of fura-2 fluorescence intensity in response to electrical stimuli (ΔFFI); (C): Single exponential fluorescence decay rate; (D): Bi-exponential fluorescence decay rate; and (F): Changes in PS in response to increased stimulus frequency (0.1 – 5.0 Hz). Each point represents PS normalized to that of 0.1 Hz of the same cell. Mean ± SEM, n = 53 cells (A-D) or 23-25 cells (E) per group, * $p < 0.05$ *vs.* FVB; # $p<0.05$ *vs.* FVB mice consuming ethanol (FVB-ETOH).

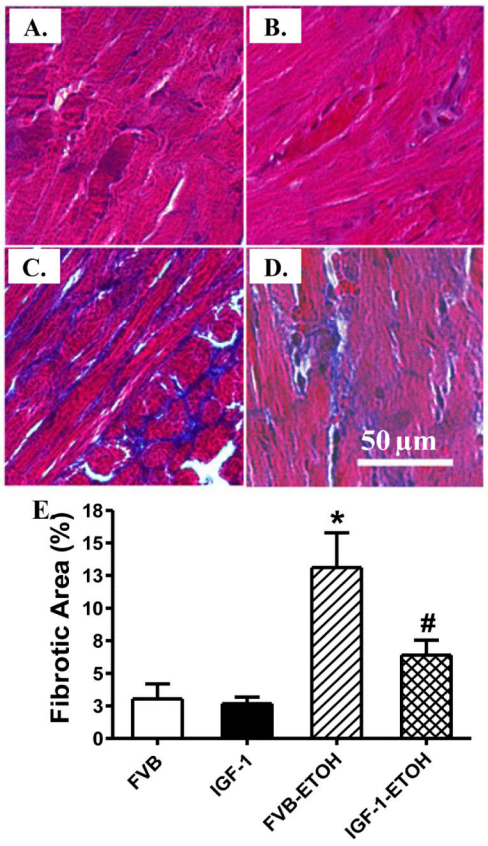

Fig. 4.

Effect of chronic alcohol intake on myocardial fibrosis in FVB and IGF-1 mice. (A-D): Representative photomicrographs (400x) of myocardial sections stained with Masson trichrome. (A): FVB; (B): IGF-1; (C): FVB-ETOH; and (D): IGF-1-ETOH; (E): Pooled data of 15 fields from 3 mice, Mean ± SEM, * $p < 0.05$ *vs.* FVB group, # $p < 0.05$ *vs.* FVB mice consuming ethanol (FVB-ETOH).

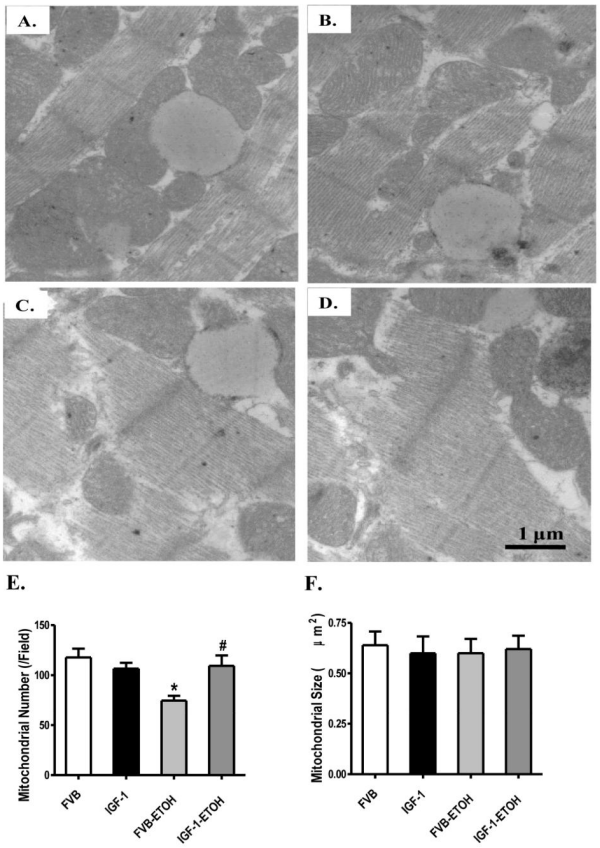

Fig. 5.

Transmission electron microscopic micrographs of left ventricular tissues from FVB or IGF-1 mice with or without chronic alcohol consumption. Panels A (FVB), B (IGF-1) and D (IGF-1-ETOH) display regular myofilament and regular mitochondrial structure whereas panel C (FVB-ETOH) displays regular myofilament associated with reduced mitochondrial number or density (10,000x). Panel E: mitochondrial density; Panel F: mitochondrial size. Mean ± SEM, n = 6-7 fields per mouse from 3 mice,* $p < 0.05$ *vs*. FVB group, # $p < 0.05$ *vs.* FVB mice consuming ethanol (FVB-ETOH) group.

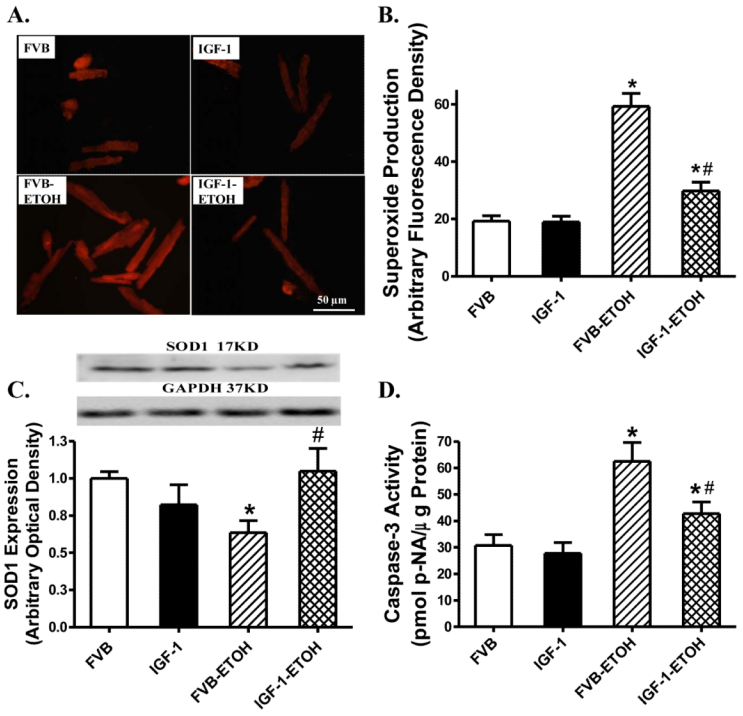

Fig. 6.

Effect of chronic alcohol intake on superoxide generation, Cu/Zn superoxide dismutase (SOD1) expression and caspase-3 activity in cardiomyocytes or myocardium from FVB and IGF-1 mice. (A): Representative DHE fluorescent images (400x) showing superoxide production in cardiomyocytes from FVB and IGF-1 mice with or without chronic alcohol intake; (B): Pooled data of superoxide production from 120-160 cells from 4 mice per group; (C): SOD1 expression. Inset: Representative gel bots of SOD1 and GAPDH (loading control) using specific antibodies; and (D): Caspase-3 activity using the colorimetric substrate Ac-DEVD-pNA. Mean ± SEM, n = 5-7 mice per group. * $p < 0.05$ *vs.* FVB; # $p < 0.05$ *vs.* FVB mice consuming ethanol (FVB-ETOH).

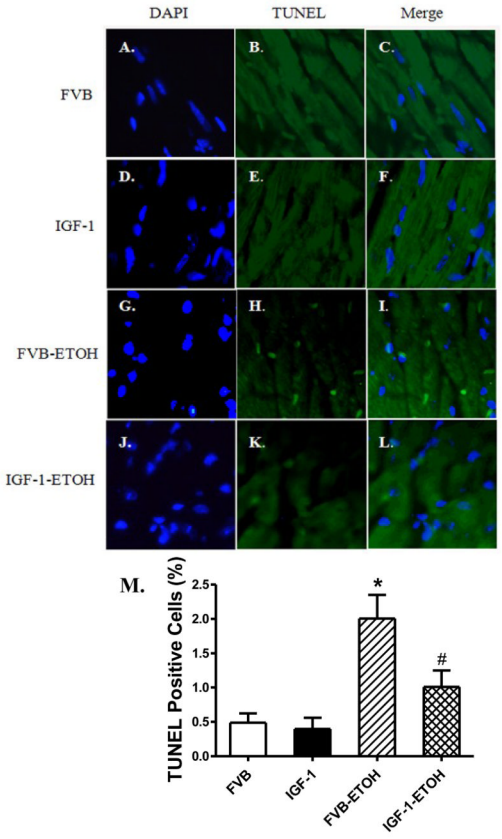

Fig. 7.

Effect of chronic alcohol intake on apoptosis using TUNEL staining in myocardium. All nuclei were stained with DAPI shown in blue in panels A (FVB), D (IGF-1), G (FVB-ETOH) and J (IGF-1-ETOH). The TUNEL-positive nuclei were visualized with fluorescein (green) in panels B (FVB), E (IGF-1) H (FVB-ETOH) and K (IGF-1-ETOH). Panels C (FVB), F (IGF-1), I (FVB-ETOH) and I (IGF-1-ETOH) depict merged DAPI and TUNEL-positive nuclei staining. Original magnification = 400×. Quantified data are shown in panel M. Mean ± SEM, n = 15 fields from 3 mice per group, * $p < 0.05$ *vs.* FVB; # $p<0.05$ *vs.* FVB mice consuming ethanol (FVB-ETOH).

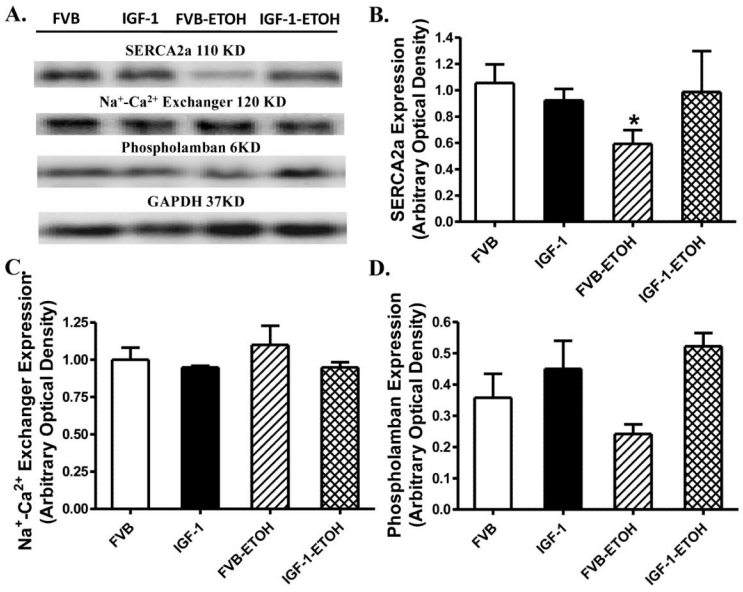

Fig. 8.

Western blot analysis of sarco(endo)plasmic reticulum Ca^{2+}-ATPase (SERCA2a), Na^{+}-Ca^{2+} exchanger and phospholamban in myocardium from FVB and IGF-1 mice with or without ethanol consumption (ETOH). (A): Representative gel blots of SERCA2a, Na^{+}-Ca^{2+} exchanger, phospholamban and GAPDH (loading control) using specific antibodies; (B): SERCA2a; (C): Na^{+}-Ca^{2+} exchanger; and (D): Phospholamban. Mean ± SEM. n = 4 – 6, * $p < 0.05$ *vs.* FVB.

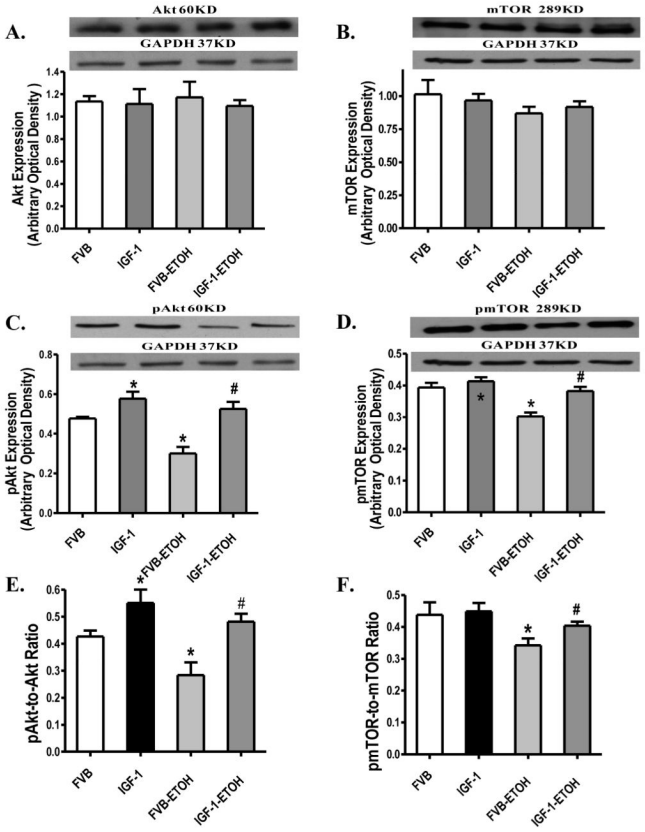

Fig. 9.

Western blot analysis of pan and phosphorylated Akt and mTOR in myocardium from FVB and IGF-1 mice with or without chronic alcohol consumption. (A): Akt; (B): mTOR; (C): Phosphorylated Akt (pAkt); (D): Phosphorylated mTOR (pmTOR); (E): pAkt-to-pan Akt ratio; and (F): pmTOR-to-pan mTOR ratio. Insets: Representative gel blots depicting expression of Akt, mTOR, pAkt, pmTOR and GAPDH (used as loading control). Mean ± SEM. n = 6 – 7, * $p < 0.05$ *vs.* FVB group, # $p < 0.05$ *vs.* FVB mice consuming ethanol (FVB-ETOH).

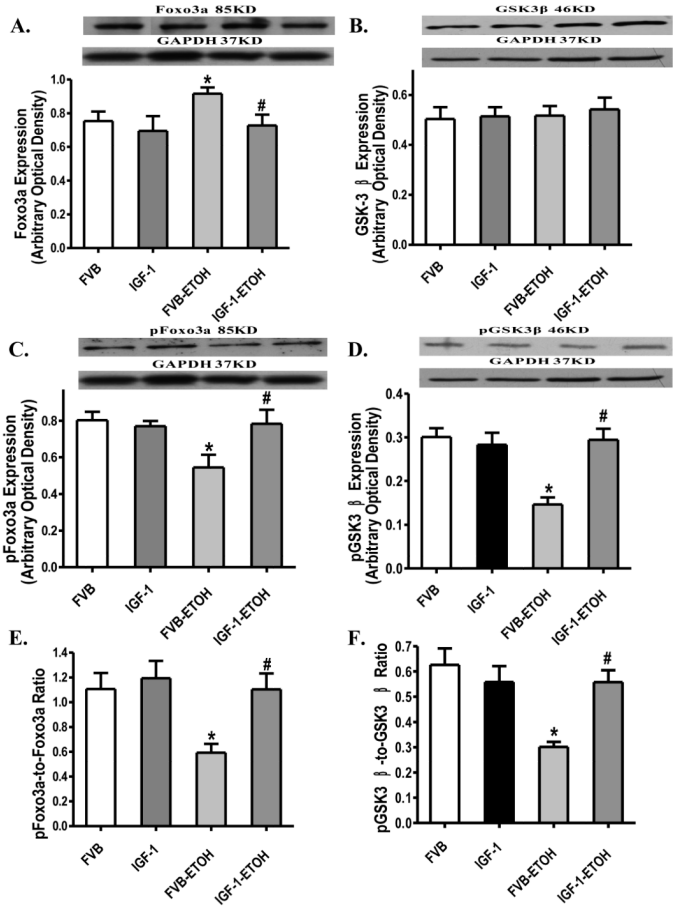

Fig. 10.

Western blot analysis of pan and phosphorylated Foxo3a and GSK3β in myocardium from FVB and IGF-1 mice with or without chronic alcohol consumption. (A): Foxo3a; (B): GSK3β; (C): Phosphorylated Foxo3a (pFoxo3a); (D): Phosphorylated GSK3β (pGSK3β); (E): pFoxo3a-to-pan Foxo3a ratio; and (F): pGSK3β-to-pan GSK3β ratio. Insets: Representative gel blots depicting expression of Foxo3a, GSK3β, pFoxo3a, pGSK3β and GAPDH (loading control). Mean ± SEM. n = 6 – 8, * $p < 0.05$ *vs.* FVB group, # $p < 0.05$ *vs.* FVB mice consuming ethanol (FVB-ETOH).

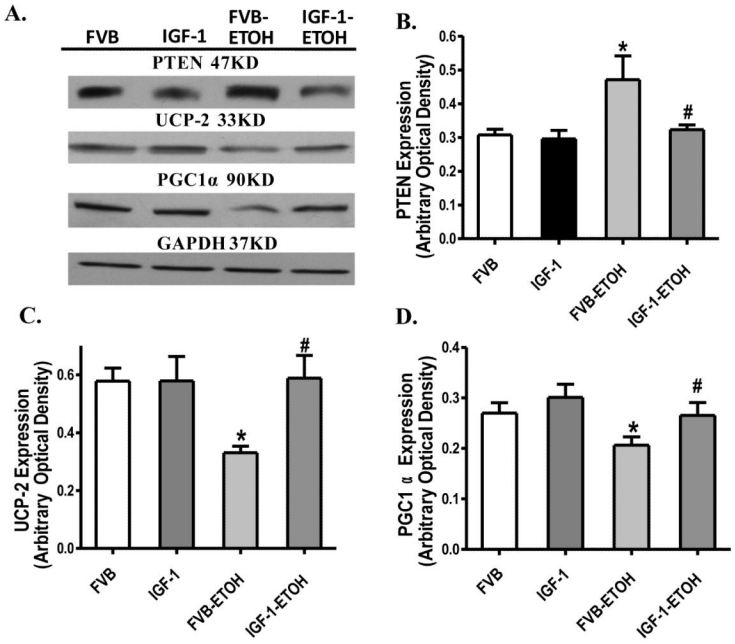

Fig. 11.

Western blot analysis of PTEN, UCP-2 and PGC1α in myocardium from FVB and IGF-1 mice with or without chronic alcohol consumption. (A): Representative gel blots of PTEN, UCP-2, PGC1α and GAPDH (loading control); (B): PTEN; (C): UCP-2; and (D): PGC1α. Mean ± SEM. n = 6 – 7, * $p < 0.05$ *vs.* FVB group, # $p < 0.05$ *vs.* FVB mice consuming ethanol (FVB-ETOH).

Table 1

Biometric parameters of mice fed an alcohol diet (4%) for 16 weeks

Parameter	FVB	IGF-1	FVB-ETOH	IGF-1-ETOH
Body Weight (g)	24.6 ± 1.3	25.0 ± 1.2	24.3 ± 1.4	24.5 ± 1.0
Heart Weight (mg)	122 ± 8	137 ± 9	156 ± 10*	154 ± 5*
Heart/Body Weight (mg/g)	4.93 ± 0.13	5.54 ± 0.32	6.55 ± 0.43*	6.35 ± 0.18*
Liver Weight (g)	1.20 ± 0.05	1.20 ± 0.05	1.28 ± 0.07	1.19 ± 0.05
Liver/Body Weight (mg/g)	48.9 ± 0.9	48.4 ± 1.3	53.2 ± 1.6	49.1 ± 1.8
Kidney Weight (g)	0.33 ± 0.02	0.34 ± 0.02	0.33 ± 0.02	0.35 ± 0.02
Kidney/Body Weight (mg/g)	13.5 ± 0.6	13.6 ± 0.5	13.7 ± 0.5	14.1 ± 0.4
Heart Rate (bpm)	482 ± 27	464 ± 23	509 ± 30	495 ± 22
Blood Alcohol (mg/dl)	Undetectable	Undetectable	162 ± 12*	180 ± 15*

ETOH = alcohol consuming; Mean ± SEM, n = 12 - 14 mice per group

* $p < 0.05$ *vs.* FVB group.